

Magnetic field penetration in a long Josephson junction imbedded in a wide stripline

Andreas Franz,^{a)} Andreas Wallraff, and Alexey V. Ustinov
Physikalisches Institut III, Universität Erlangen-Nürnberg, D-91058 Erlangen, Germany

(Received 14 April 2000; accepted for publication 21 September 2000)

The dependence of the first critical field of long linear and annular Josephson junctions on the width of the surrounding stripline, the so called idle region, is investigated experimentally. The stripline modifies the effective Josephson length λ_{eff} in the junction. The experimental data are compared with the theory by Caputo *et al.* [J. Appl. Phys. **85**, 7291 (1999)] and good agreement is found. The dependence of the first critical field on the width of the surrounding stripline can be well explained using the same λ_{eff} for both annular and linear junctions. © 2001 American Institute of Physics. [DOI: 10.1063/1.1325006]

I. INTRODUCTION

A Josephson junction is formed by two superconductors separated by a thin oxide layer allowing the tunneling of electrons.^{1–3} Long Josephson junctions, i.e., junctions with one dimension larger than the Josephson length λ_J ,³ are of interest for both basic and applied physics. Long Josephson junctions offer the possibility of studying solitons that account for magnetic flux quanta moving along the tunnel barrier.⁴ Long annular Josephson junctions are especially unique devices for this purpose, because they allow for solitons to be studied without collisions with boundaries.⁵ Solitons can be trapped, e.g., during the normal–superconducting transition. In the superconducting state trapped solitons cannot disappear and only soliton–antisoliton pairs can be created.⁶ If only one soliton is trapped in an annular junction, it will suffer neither boundary reflections nor collision with other solitons, so unperturbed soliton motion can be studied.⁶ A Josephson soliton is—among other properties—an electromagnetic pulse. When solitons arrive periodically at the free end of a linear junction, radiation in the microwave or millimeter-wave region of the electromagnetic spectrum is emitted, which leads to applications of long Josephson junctions as oscillators.⁷

The maximum possible superconducting current, that is the critical current I_c , of a Josephson junction depends on the external magnetic field.^{2,3,8} In weak magnetic fields long Josephson junctions behave like weak superconductors and show the Meissner effect.⁹ In this regime the critical current decreases linearly with the external field.¹⁰ This behavior exists until a critical field H_{c_1} is reached. At this field solitons in the form of magnetic fluxons can overcome the edge barrier and penetrate into the junction.¹⁰ For a long linear Josephson junction the first critical field is⁹

$$H_{c_1} = \frac{\Phi_0}{\pi \Lambda \lambda_J}, \quad (1)$$

where $\Lambda = \lambda_{L_b} \tanh(d_b/2\lambda_{L_b}) + \lambda_{L_t} \tanh(d_t/2\lambda_{L_t}) + t$ is the ef-

fective magnetic thickness of the junction,¹¹ and λ_{L_b} and λ_{L_t} are the London penetration depths of the bottom and top electrode of the junction, respectively. The thicknesses of the bottom and top electrode and of the tunnel barrier are d_b , d_t , and t , respectively. The Josephson length is given by³

$$\lambda_J = \sqrt{\frac{\Phi_0}{2\pi j_c \mu_0 d'}}, \quad (2)$$

where Φ_0 is the flux quantum, j_c is the critical current density, and $d' = \lambda_{L_b} \coth(d_b/\lambda_{L_b}) + \lambda_{L_t} \coth(d_t/\lambda_{L_t}) + t$.¹¹

Typical fabrication processes for high quality Josephson tunnel junctions in Nb/Al technology use anodic oxidation or SiO_x deposition for insulation. This leads to an overlap between the lower and upper electrode, resulting from the oversized dimensions of the Nb layers.^{12,13} To avoid short circuits the two electrodes are separated by an insulator that is thicker than the junction barrier. This part of the junction, called the passive or idle region because no tunneling through it is possible, forms a superconducting stripline surrounding the Josephson junction. A Josephson junction with an idle region is also often called a window junction. Window junctions have an advantage over ordinary junctions because of a more uniform and better controlled oxide barrier.¹⁴

The idle region affects both the dynamic and static properties of the Josephson junctions.^{12,13,15–24} In this article we investigate experimentally the influence of the width of the idle region on the critical current versus magnetic field dependence of long linear and annular Josephson junctions and compare our data with the existing theory.^{21,23} In Sec. II experimental data for linear (straight) and annular (ring-shaped) junctions with various idle regions are presented. These data are compared with theoretical predictions in Sec. III. The dependence of the first critical field for long linear Josephson junctions has been studied before^{12,13,15} but not compared with theory because, at the time when the data were obtained, the theory was not yet completely developed. For annular Josephson junctions the dependence of the critical field on the idle region has not been studied until now.

^{a)} Author to whom correspondence should be addressed; electronic mail: franz@physik.uni-erlangen.de

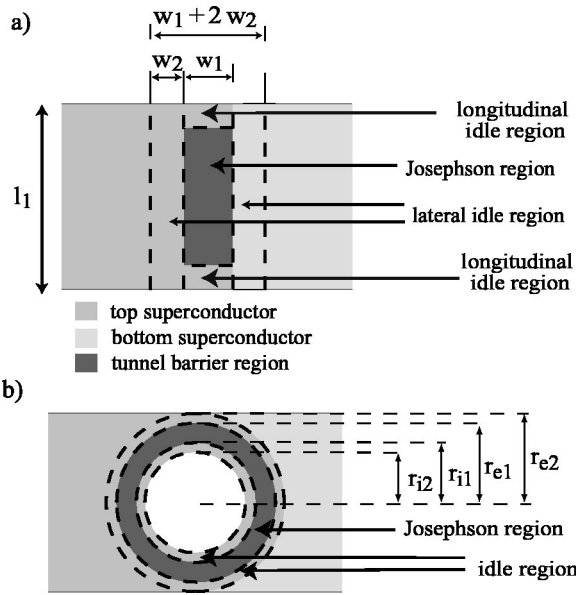


FIG. 1. Top view of a linear (a) and an annular Josephson junction (b) with symmetric idle region.

A schematic top view of a linear junction with symmetric lateral and longitudinal idle areas is shown in Fig. 1(a). In Fig. 1(b) a top view of an annular junction with a symmetric idle region is shown. In the following all quantities related to the active Josephson region are labeled with an index 1, and all quantities related to the passive idle region are labeled with an index 2. For an annular junction with a symmetric idle region the junction width is given by $w_1 = r_{e1} - r_{i1}$ and the idle width is given by $w_2 = r_{e2} - r_{e1} = r_{i1} - r_{i2}$.

A cross section in the direction perpendicular to the long dimension of a junction with an idle region is shown in Fig. 2. Here, $t_{1/2}$ is the thickness of the insulator in the Josephson and the idle regions, respectively; $\epsilon_{1/2}$ is the relative dielectric constant of the two barriers, respectively.

Lateral and longitudinal idle areas play different roles for long linear junctions.¹⁹ The lateral idle region leads to an increase of the velocity of linear waves,¹⁷⁻¹⁹ while the longitudinal passive region acts as a lumped capacitance that

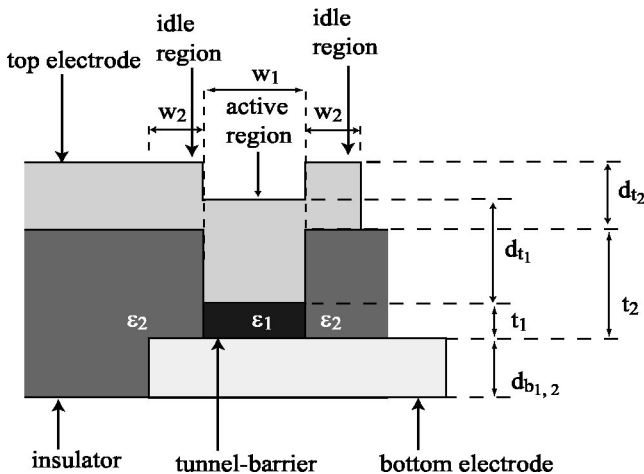


FIG. 2. Cross section of a Josephson junction with idle region.

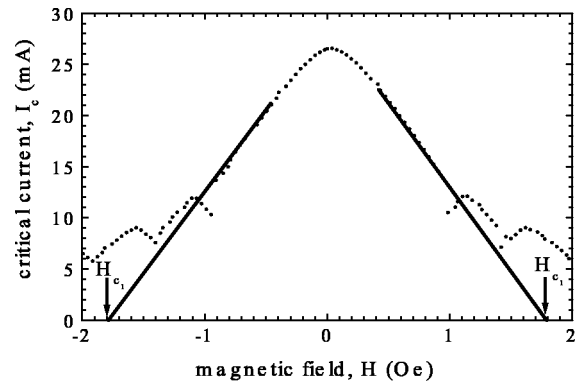


FIG. 3. Determination of the first critical field H_{c1} from experimental data. The data are taken from the annular Josephson junction ANN2E with $w_1 = 6 \mu\text{m}$ and $w_2 = 22 \mu\text{m}$ (see Table II).

loads the Josephson junction.¹⁹ The lateral idle area also introduces an effective Josephson length, which is due to a rescaling of the Josephson length of a bare junction.²¹

The effective Josephson length for a junction with small lateral idle regions was calculated in Ref. 21 using a variational approach for the free energy. The result obtained is

$$\lambda_{\text{eff}} = \lambda_J \sqrt{1 + \frac{2w_2 L_1^*}{w_1 L_2^*}}, \quad (3)$$

where L_1^* and L_2^* are the specific inductances of the active and passive regions, respectively, with $L_i^* = \mu_0 d_i'$. Equation (3) can be easily understood by considering a parallel combination of the inductances per unit length $L_i = 1/w_i L_i^*$ of the junction and stripline with the total inductance $1/L_{\text{tot}} = 1/L_1 + 2/L_2$. The factor 2 appears because the size of the idle regions is w_2 on both sides of the active region and, thus, the total width of idle region is $2w_2$.

In Ref. 21 the critical current diffraction patterns (magnetic field dependencies of the critical current) for linear junctions with small idle regions were calculated numerically and compared with the calculation from Ref. 10 for a junc-

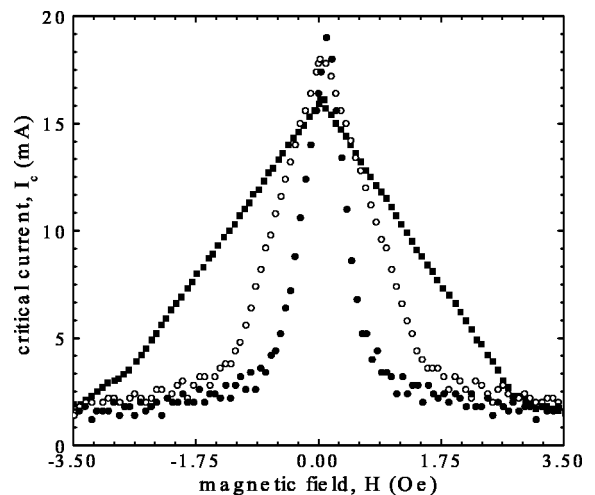


FIG. 4. Critical current diffraction patterns of three linear Josephson junctions with $l_1 = 350 \mu\text{m}$ and $w_1 = 20 \mu\text{m}$. The idle size is $w_2 = 10 \mu\text{m}$ (LIN1A, squares), $w_2 = 60 \mu\text{m}$ (LIN1C, open circles) and $w_2 = 150 \mu\text{m}$ (LIN1E, closed circles).

TABLE I. Dimensions and effective Josephson length of the linear Josephson junctions after Eq. (3) with $l_1 = 350 \mu\text{m}$, $w_1 = 20 \mu\text{m}$ (set LIN1) and $l_1 = 450 \mu\text{m}$, $w_1 = 10 \mu\text{m}$ (set LIN2).

Junction No.	LIN1					LIN2			
	A	B	C	D	E	A	B	C	D
$w_2 (\mu\text{m})$	10	30	60	100	150	30	60	100	150
w_2/w_1	0.5	1.5	3.0	5.0	7.5	3.0	6.0	10.0	15.0
$\lambda_{\text{eff}}/\lambda_J$	1.3	1.7	2.2	2.8	3.3	2.3	3.1	3.9	4.7

tion with the same dimensions but without an idle region. A good agreement was found by substituting λ_{eff} instead of λ_J into Eq. (1). Numerical simulation shows that H_{c_1} decreases inversely as λ_{eff} .²³ In Ref. 22 the critical current diffraction patterns of short linear junctions were investigated experimentally and the rescaling of the Josephson length was found intuitively.

II. EXPERIMENTAL DATA

From the experimental data the first critical field is determined by linearly extrapolating the branch starting at the maximum zero field critical current to $I=0$, as shown in Fig. 3. The decrease of the first critical field H_{c_1} in the presence of an idle region was first observed experimentally for long linear Josephson junctions by Thyssen *et al.*^{12,13} In Fig. 4 the diffraction patterns of three linear junctions of the same length $l_1 = 350 \mu\text{m}$ and width $w_1 = 20 \mu\text{m}$ but different idle widths $w_2 = 10 \mu\text{m}$, $w_2 = 60 \mu\text{m}$, and $w_2 = 150 \mu\text{m}$ are shown. These data are taken from Ref. 15.

It is observed that the critical current at zero field increases with increasing idle region.^{12,13} This effect can be explained by a more homogeneous current distribution due to the idle region, which reduces the self field generated by the bias current.¹⁵

Similar behavior is also observed in our measurements of annular Josephson junctions presented below. With increasing idle width w_2 the first critical field decreases and the critical current at zero field increases. Figure 5 shows the diffraction patterns of two annular Josephson junctions with different idle widths.

To systematically study the influence of the idle region on the diffraction patterns two series of linear and two series of annular junctions were measured (see Tables I and II). In

each series all parameters are the same, except for the width of the idle region w_2 , which is varied. All annular junctions were prepared on the same chip using Hypres²⁵ technology with a nominal critical current density of 1000 A/cm^2 . Accordingly, the Josephson length is approximately $10 \mu\text{m}$ at 4.2 K. In the linear junctions of the set LIN1 the critical current density is $j_c = 245 \text{ A/cm}^2$ and thus $\lambda_J = 20 \mu\text{m}$; in the set LIN2 $j_c = 210 \text{ A/cm}^2$ and thus $\lambda_J = 21 \mu\text{m}$.¹⁵

All samples were measured directly in a bath of liquid helium at a temperature of 4.2 K using battery powered current sources for the bias current and magnetic field. The junctions were surrounded by a cryoperm shield for protection against external magnetic fields. Inside the shield a coil was used for applying a magnetic field. The magnetic field was parallel to the bias leads.

The dependence of the first critical field on the idle width for the two sets LIN1 and LIN2 of linear junctions is shown in the inset of Fig. 6. According to the theory of Caputo *et al.*^{21,23} in the limit of the small idle region, the first critical field should depend only on the ratio w_2/w_1 . This is confirmed by our experiments. Plotting the measured critical field of the two sets LIN1 and LIN2 against the ratio w_2/w_1 , all data points lie within the experimental error on a single curve (see Fig. 6). Thus, no geometrical effect on H_{c_1} other than the ratio of w_2/w_1 is evident.

The dependence of the first critical field on the width of the idle region $H_{c_1}(w_2)$ is shown for the annular junctions in the inset of Fig. 7. Again we find a strong dependence of H_{c_1} on the idle width, similar to that for linear junctions. Plotting $H_{c_1}(w_2)$ against the ratio w_2/w_1 , one finds that all data points show, within the experimental error, a universal de-

TABLE II. Dimensions and effective Josephson length of the annular junctions after Eq. (3) with mean radius $\bar{r} = (r_{e1} + r_{i1})/2 = 55 \mu\text{m}$ and Josephson length $\lambda_J \approx 10 \mu\text{m}$ and width $w_1 = 10 \mu\text{m}$ (set ANN1) and width $w_1 = 6 \mu\text{m}$ (set ANN2).

Junction No.	ANN1						ANN2				
	A	B	C	D	E	F	A	B	C	D	E
$w_2 (\mu\text{m})$	3	5	10	15	20	30	3	5	7	12	22
w_2/w_1	0.3	0.5	1.0	1.5	2.0	3.0	0.5	0.83	1.17	2.0	3.67
$\lambda_{\text{eff}}/\lambda_J$	1.16	1.25	1.47	1.65	1.82	2.11	1.25	1.40	1.53	1.82	2.28

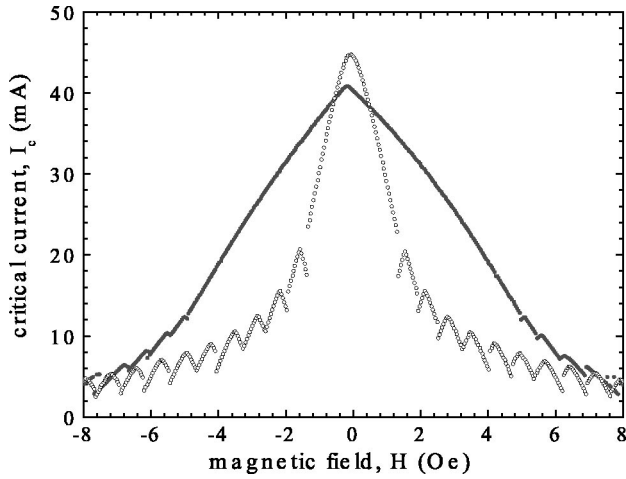


FIG. 5. Critical current diffraction patterns of two annular junctions with $r_{e1} = 60 \mu\text{m}$ and $w_1 = 10 \mu\text{m}$. The idle widths $w_2 = 3 \mu\text{m}$ (ANN1A, closed circles) and $w_2 = 30 \mu\text{m}$ (ANN1F, open circles).

pendence on this ratio, as can be seen from Fig. 7. Therefore, in the limit of small idle width the first critical field depends only on the ratio of w_2/w_1 for annular Josephson junctions with the same mean radius \bar{r} .

III. COMPARISON BETWEEN THEORY AND EXPERIMENT

It has been shown by Caputo *et al.*^{21,23} that the idle region introduces an effective Josephson length λ_{eff} and that the first critical field decreases inversely proportional to λ_{eff} .²³

$$H_{c1} \propto \frac{1}{\lambda_{\text{eff}}}. \tag{4}$$

In Ref. 23 the effective Josephson length has been calculated numerically for different idle widths w_2 . The starting point

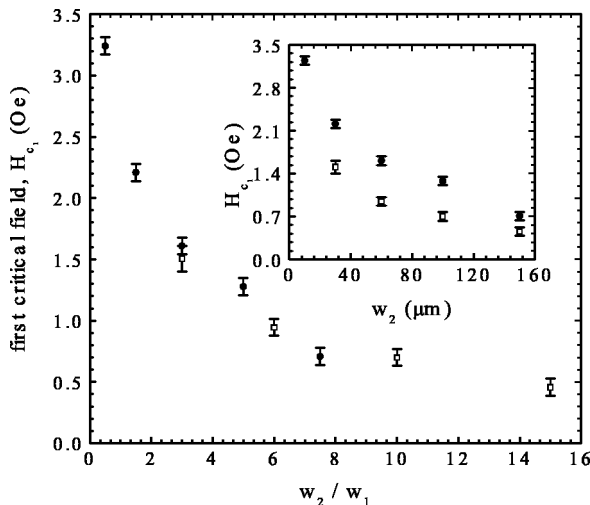


FIG. 6. Dependence of the first critical field on the ratio of the idle width to the junction width w_2/w_1 for the two series of linear junctions LIN1 (dark circles) and LIN2 (open squares). The inset shows the dependence of first critical field on w_2 for the same junctions.

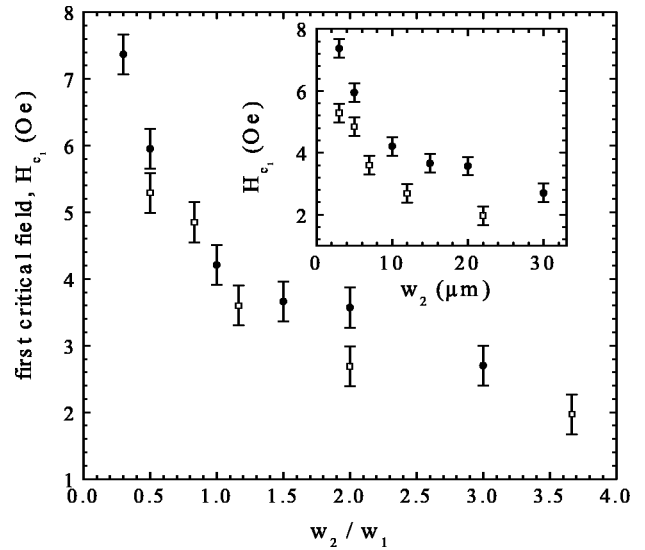


FIG. 7. Dependence of the first critical field on the ratio w_2/w_1 for both annular junction series ANN1 (dark circles) and ANN2 (open squares). The inset shows the dependence of the first critical field on w_2 for the same junctions.

is the system of partial differential equations describing the static properties of a Josephson junction with an idle region

$$\Delta \phi = \sin \phi, \tag{5a}$$

$$\Delta \psi = 0, \tag{5b}$$

where ϕ and ψ are the phase differences in the junction and idle region, respectively. Equations (5a) and (5b) are coupled via the boundary conditions. The boundary conditions between active and passive region are²³

$$\phi = \psi \tag{6a}$$

and

$$\frac{\partial \psi}{\partial n} = \frac{L_2^*}{L_1^*} \frac{\partial \phi}{\partial n} \tag{6b}$$

and on the external surface

$$\frac{\partial \psi}{\partial n} = L_2^* I_{\text{ext}} \frac{\lambda_J}{\Phi_0}, \tag{7}$$

where $\partial/\partial n$ is the outward normal derivative and I_{ext} is due to the external bias current or the applied magnetic field. From these equations one can obtain a one-dimensional (1D) integro-differential equation by assuming a narrow window and integrating the 2D sine-Gordon equation over the width of the window.²³ Supposing that the phase does not vary over the size w_1 , it can be integrated over the window and will only depend on the x dimension

$$\varphi(x) = \frac{1}{w_1} \int_{-w/2}^{w/2} \phi(x,y) dy. \tag{8}$$

In the limit of small idle width, the integro-differential equation obtained reduces to²³

$$-\lambda_{\text{eff}}^2 \frac{\partial^2 \varphi}{\partial x^2} + \sin \varphi = 0, \tag{9}$$

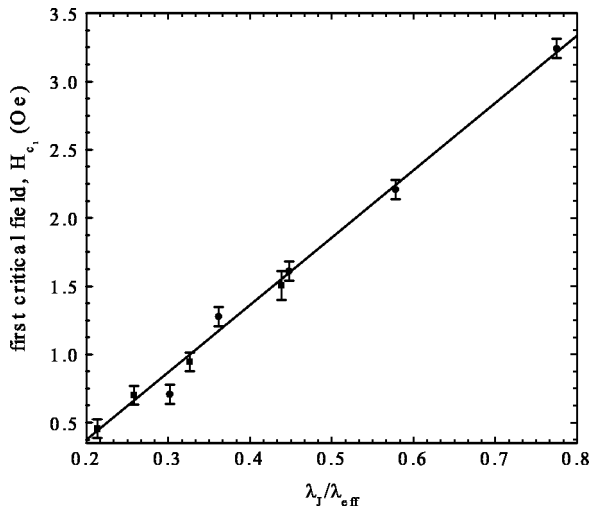


FIG. 8. First critical field vs reciprocal normalized effective Josephson length for the two sets of linear junctions LIN1 (circles) and LIN2 (squares). The straight line is a linear fit to all data points.

where λ_{eff} is given by Eq. (3). For larger idle width the resulting integro-differential equation is calculated from a variation of the free energy.²³ In the case of infinitive idle width ($w_2 \rightarrow \infty$) the effective Josephson length is²¹

$$\lambda_{\text{eff}} = \lambda_J \frac{\pi}{2} \frac{L_1^*}{L_2^*} \frac{\lambda_J}{w_1} \left(1 + \sqrt{1 + \frac{4w_1^2}{\pi^2 \lambda_J^2} \left(\frac{L_2^*}{L_1^*} \right)^2} \right). \quad (10)$$

No analytical expression for λ_{eff} exists for arbitrary idle width and the effective Josephson length has to be calculated numerically in such a case. The prediction of Eq. (4) can be checked by plotting the first critical field versus the reciprocal normalized effective Josephson length for all measured junctions. From Eq. (3) it follows that the effective Josephson length, in the limit of small idle width, and thus also H_{c1} , depend only on the ratio w_2/w_1 . In Fig. 8 the first critical field is plotted versus the reciprocal normalized effective Josephson length for the two sets of linear junctions from Ref. 15. The straight line in Fig. 8 is a linear fit of all data points. The standard deviation in the fit is about 3%.

In the following we apply the theory^{21,23} developed for linear junctions to annular junctions. The first critical field for the two sets of annular junctions ANN1 and ANN2 is plotted in Fig. 9 versus the reciprocal normalized effective Josephson length calculated from Eq. (3). The standard deviation of the fit is about 10%. It can be seen from Fig. 9 that for annular Josephson junctions with small idle region the effective Josephson length also seems to be well described by Eq. (3). The dependence of the first critical field on the ratio w_2/w_1 should be explained by the same theory as for linear junctions.²⁶ The reason is that the Josephson region $w_1 < \lambda_J$ can be viewed as one dimensional and the universal scaling must persist.

In Ref. 23 λ_{eff} has been calculated only for the inductance ratio $L_2^*/L_1^* = 1$. The two limiting cases, Eqs. (3) and (10), have been calculated in Ref. 21 for arbitrary inductance ratio. For our junctions the inductance ratio is about 1.7. For larger but not infinitive idle regions a second order correction should be taken into account.²⁷ As mentioned before, Eq. (3)

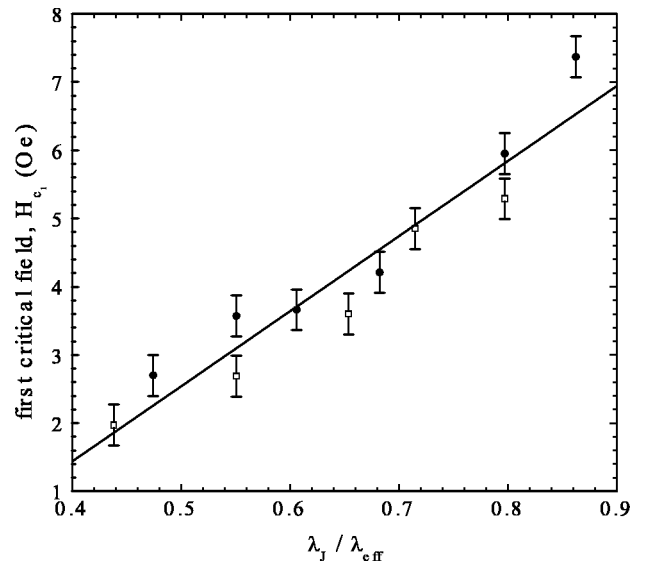


FIG. 9. First Critical field vs reciprocal normalized effective Josephson length for the two series of annular junctions ANN1 (circles) and ANN2 (squares). The straight line is a linear fit to all data points. The error of the fit is about 1.3 Oe.

is derived as a limiting case for small idle regions.^{21,23} It is not possible to give an analytic expression for arbitrary idle regions. From the integro-differential equation²³ the second order correction for the effective Josephson length λ_{eff} is given by the implicit formula²⁷

$$\lambda_{\text{eff}} = \lambda_J \sqrt{1 + \frac{2w_2}{w_1} \frac{L_1^*}{L_2^*} \left(1 - \left(\frac{w_2}{2\pi\lambda_{\text{eff}}} \right)^2 \right)}. \quad (11)$$

We have calculated the first and second order corrections for the annular junctions ANN1. The largest idle width from this series is $w_2 = 30 \mu\text{m}$. As can be seen from Fig. 10, the second order correction for this value of w_2 is about 2% and thus smaller than the experimental uncertainty and, therefore, cannot be seen in the experimental data. The same is valid for all other junctions used in our experiments.

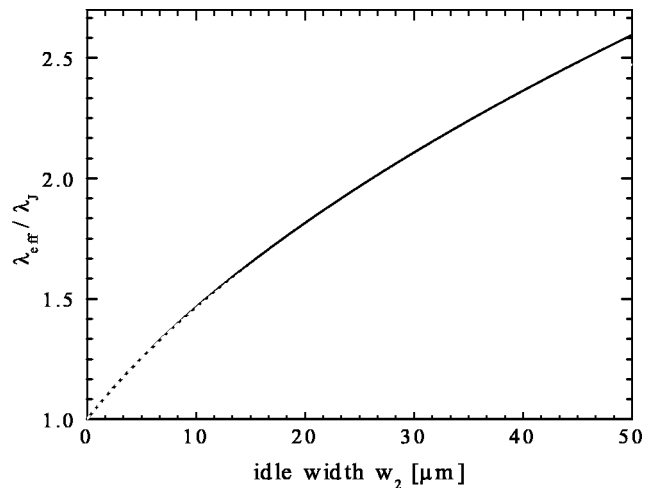


FIG. 10. First order (solid line) and second order (dashed line) correction for λ_J vs the width of the idle region w_2 , calculated with the parameters of our annular junctions with $r_{e1} = 60 \mu\text{m}$ and $w_1 = 10 \mu\text{m}$ (ANN1).

IV. SUMMARY AND CONCLUSION

The presence of an idle region changes the effective Josephson length by a large factor. Thus, the idle region drastically changes the static and dynamic properties of long Josephson junctions. The dependence of the measured first critical field on the idle region size for long Josephson junctions is well explained by using the effective Josephson length λ_{eff} instead of λ_J as predicted in Refs. 21 and 23. The first critical field decreases inversely as the effective Josephson length. We have found excellent agreement between experiment and theory for both linear and annular Josephson junctions.

ACKNOWLEDGMENTS

The authors would like to thank J.-G. Caputo and V. V. Kurin for useful discussions, and also acknowledge N. Thyssen for data on linear junctions.

¹B. D. Josephson, Phys. Lett. **1**, 251 (1962).

²B. D. Josephson, Rev. Mod. Phys. **36**, 216 (1964).

³A. Barone and G. Paterno, *Physics and Applications of the Josephson Effect* (Wiley, New York, 1982).

⁴A. V. Ustinov, Physica D **123**, 315 (1998).

⁵D. W. McLaughlin and A. C. Scott, Phys. Rev. A **18**, 1652 (1978).

⁶A. Davidson, B. Dueholm, B. Kryger, and N. F. Pedersen, Phys. Rev. Lett. **55**, 2059 (1985).

⁷R. D. Parmentier, in *The New Superconducting Electronics*, edited by H. Weinstock and R. W. Ralston (Kluwer, Dordrecht, 1993), pp. 221–248.

⁸J. M. Rowell, Phys. Rev. Lett. **11**, 200 (1963).

⁹K. Schwidtal, Phys. Rev. B **2**, 2526 (1970).

¹⁰C. S. Owen and D. J. Scalapino, Phys. Rev. **164**, 538 (1967).

¹¹M. Weihnacht, Phys. Status Solidi **32**, K169 (1969).

¹²N. Thyssen *et al.*, in *Nonlinear Superconducting Devices and High- T_c Materials*, edited by R. D. Parmentier and N. F. Pedersen (World Scientific, Singapore, 1995), pp. 115–125.

¹³N. Thyssen *et al.*, IEEE Trans. Appl. Supercond. **5**, 2965 (1995).

¹⁴W. Schroen and J. P. Pritchard, Jr., J. Appl. Phys. **40**, 2118 (1969).

¹⁵N. Thyssen, Masters thesis, Mathematisch—Naturwissenschaftliche Fakultät der Rheinisch-Westfälischen Technischen Hochschule Aachen, 1995.

¹⁶J. G. Caputo, N. Flytzanis, and M. Devoret, Phys. Rev. B **50**, 6471 (1994).

¹⁷G. S. Lee, IEEE Trans. Appl. Supercond. **1**, 121 (1991).

¹⁸G. S. Lee and A. T. Barfknecht, IEEE Trans. Appl. Supercond. **2**, 67 (1992).

¹⁹R. Monaco, G. Costabile, and N. Martucciello, J. Appl. Phys. **77**, 2073 (1995).

²⁰J.-G. Caputo, N. Flytzanis, and E. Vavalis, Int. J. Mod. Phys. C **6**, 241 (1995).

²¹J.-G. Caputo, N. Flytzanis, and E. Vavalis, Int. J. Mod. Phys. C **7**, 191 (1996).

²²S. Maggi and V. Lacquaniti, J. Low Temp. Phys. **106**, 393 (1997).

²³J.-G. Caputo *et al.*, J. Appl. Phys. **85**, 7291 (1999).

²⁴A. Wallraff, Physica B **284-286**, 575 (2000).

²⁵Hypres Inc., Elmsford, NY 10523.

²⁶J.-G. Caputo (private communication).

²⁷V. V. Kurin (private communication).